

Doped polymer for low-loss dielectric material in the terahertz range

Daniel Headland,^{1,4} Peter Thurgood,² Daniel Stavrevski,² Withawat Withayachumnankul,^{1,2,3} Derek Abbott,¹ Madhu Bhaskaran,² and Sharath Sriram^{2,5}

¹*School of Electrical & Electronic Engineering, The University of Adelaide, SA 5005, Australia*

²*Functional Materials and Microsystems Research Group, RMIT University, Melbourne, VIC 3001, Australia*

³*Interdisciplinary Graduate School of Science and Engineering, Tokyo Institute of Technology, Ookayama, Meguro-ku, Tokyo 152-8552, Japan*

⁴daniel.headland@adelaide.edu.au

⁵sharath.sriram@gmail.com

Abstract: The dielectric properties of an elastomeric polymer are modified with the inclusion of dopants, with the aim of reducing dielectric loss in the terahertz range. Polydimethylsiloxane (PDMS) is selected as the host polymer, and micro/nano-particle powders of either alumina or polytetrafluoroethylene (PTFE) are employed as dopants. Composite samples are prepared, and characterised with terahertz time-domain spectroscopy (THz-TDS). The samples exhibit significantly reduced dielectric loss, with a maximum reduction of 15.3% in loss tangent reported for a sample that is 40% PTFE by mass. Results are found to have reasonable agreement with the Lichtenecker logarithmic mixture formula, and any deviation can be accounted for by agglomeration of dopant micro/nano-particles. The new dielectric composites are promising for devising efficient micro-structure components at terahertz frequencies.

© 2015 Optical Society of America

OCIS codes: (300.6495) Terahertz spectroscopy; (310.3840) Materials and process characterization; (160.5470) Polymers.

References and links

1. J. Lötters, W. Olthuis, P. Veltink, and P. Bergveld, "The mechanical properties of the rubber elastic polymer polydimethylsiloxane for sensor applications," *J. Micromech. Microeng.* **7**, 145 (1997).
2. T. Niu, W. Withayachumnankul, B. S.-Y. Ung, H. Menekse, M. Bhaskaran, S. Sriram, and C. Fumeaux, "Experimental demonstration of reflectarray antennas at terahertz frequencies," *Opt. Express* **21**, 2875–2889 (2013).
3. T. Niu, W. Withayachumnankul, A. Upadhyay, P. Gutruf, D. Abbott, M. Bhaskaran, S. Sriram, and C. Fumeaux, "Terahertz reflectarray as a polarizing beam splitter," *Opt. Express* **22**, 16148–16160 (2014).
4. Y. Z. Cheng, W. Withayachumnankul, A. Upadhyay, D. Headland, Y. Nie, R. Z. Gong, M. Bhaskaran, S. Sriram, and D. Abbott, "Ultrabroadband reflective polarization convertor for terahertz waves," *Appl. Phys. Lett.* **105**, 181111 (2014).
5. N. K. Grady, J. E. Heyes, D. R. Chowdhury, Y. Zeng, M. T. Reiten, A. K. Azad, A. J. Taylor, D. A. Dalvit, and H.-T. Chen, "Terahertz metamaterials for linear polarization conversion and anomalous refraction," *Science* **340**, 1304–1307 (2013).
6. M. Li, J. Xiao, J. Wu, R.-H. Kim, Z. Kang, Y. Huang, and J. A. Rogers, "Mechanics analysis of two-dimensionally prestrained elastomeric thin film for stretchable electronics," *Acta Mech. Solida Sin.* **23**, 592–599 (2010).
7. R. Yahiaoui, K. Takano, F. Miyamaru, M. Hangyo, and P. Mounaix, "Terahertz metamolecules deposited on thin flexible polymer: design, fabrication and experimental characterization," *J. Opt.* **16**, 094014 (2014).

8. H. Tanoto, L. Ding, and J. Teng, "Tunable terahertz metamaterials," *IEEE Trans. Terahertz Sci. Technol.* **6**, 1–25 (2013).
9. J. Li, C. M. Shah, W. Withayachumnankul, B. S.-Y. Ung, A. Mitchell, S. Sriram, M. Bhaskaran, S. Chang, and D. Abbott, "Mechanically tunable terahertz metamaterials," *Appl. Phys. Lett.* **102**, 121101 (2013).
10. K. Iwaszczuk, A. C. Strikwerda, K. Fan, X. Zhang, R. D. Averitt, and P. U. Jepsen, "Flexible metamaterial absorbers for stealth applications at terahertz frequencies," *Opt. Express* **20**, 635–643 (2012).
11. I. Khodasevych, C. M. Shah, S. Sriram, M. Bhaskaran, W. Withayachumnankul, B. S. Y. Ung, H. Lin, W. Rowe, D. Abbott, and A. Mitchell, "Elastomeric silicone substrates for terahertz fishnet metamaterials," *Appl. Phys. Lett.* **100**, 061101 (2012).
12. M. Choi, S. H. Lee, Y. Kim, S. B. Kang, J. Shin, M. H. Kwak, K.-Y. Kang, Y.-H. Lee, N. Park, and B. Min, "A terahertz metamaterial with unnaturally high refractive index," *Nature* **470**, 369–373 (2011).
13. N. Han, Z. Chen, C. Lim, B. Ng, and M. Hong, "Broadband multi-layer terahertz metamaterials fabrication and characterization on flexible substrates," *Opt. Express* **19**, 6990–6998 (2011).
14. H. Tao, C. Bingham, A. Strikwerda, D. Pilon, D. Shrekenhamer, N. Landy, K. Fan, X. Zhang, W. Padilla, and R. Averitt, "Highly flexible wide angle of incidence terahertz metamaterial absorber: Design, fabrication, and characterization," *Phys. Rev. B* **78**, 241103 (2008).
15. H. Tao, A. Strikwerda, K. Fan, C. Bingham, W. Padilla, X. Zhang, and R. Averitt, "Terahertz metamaterials on free-standing highly-flexible polyimide substrates," *arXiv preprint arXiv:0808.0454* (2008).
16. Q. Tang, M. Liang, Y. Lu, P. K. Wong, G. J. Wilmink, and H. Xin, "Development of terahertz (THz) microfluidic devices for lab-on-a-chip applications," in *Proc. SPIE Terahertz and Ultrashort Electromagnetic Pulses for Biomedical Applications*, **8585**, art. no. 858506 (San Francisco, California, 2013).
17. S. Walia, C. M. Shah, P. Gutruf, H. Nili, D. R. Chowdhury, W. Withayachumnankul, M. Bhaskaran, and S. Sriram, "Flexible metasurfaces and metamaterials: A review of materials and fabrication processes at micro-and nano-scales," *Appl. Phys. Rev.* **2**, 011303 (2015).
18. Y.-S. Jin, G.-J. Kim, and S.-G. Jeon, "Terahertz dielectric properties of polymers," *J. Korean Phys. Soc.* **49**, 513–517 (2006).
19. R. H. Giles, A. Gatesman, J. Fitzgerald, S. Fisk, and J. Waldman, "Tailoring artificial dielectric materials at terahertz frequencies," in *Proc. of the Fourth International Symposium of Space THz Technology*, 124 (Los Angeles, CA, 1993).
20. B. Ung, A. Dupuis, K. Stoeffler, C. Dubois, and M. Skorobogatiy, "High-refractive-index composite materials for terahertz waveguides: trade-off between index contrast and absorption loss," *J. Opt. Soc. Am. B* **28**, 917–921 (2011).
21. M. Scheller, S. Wietzke, C. Jansen, and M. Koch, "Modelling heterogeneous dielectric mixtures in the terahertz regime: a quasi-static effective medium theory," *J. Phys. D Appl. Phys.* **42**, 065415 (2009).
22. C. Jansen, S. Wietzke, V. Astley, D. M. Mittleman, and M. Koch, "Mechanically flexible polymeric compound one-dimensional photonic crystals for terahertz frequencies," *Appl. Phys. Lett.* **96**, 111108 (2010).
23. S. Wietzke, C. Jansen, F. Rutz, D. Mittleman, and M. Koch, "Determination of additive content in polymeric compounds with terahertz time-domain spectroscopy," *Polym. Test.* **26**, 614–618 (2007).
24. P. D. Cunningham, N. N. Valdes, F. A. Vallejo, L. M. Hayden, B. Polishak, X.-H. Zhou, J. Luo, A. K.-Y. Jen, J. C. Williams, and R. J. Twieg, "Broadband terahertz characterization of the refractive index and absorption of some important polymeric and organic electro-optic materials," *J. Appl. Phys.* **109**, 043505–043505 (2011).
25. K. Berdel, J. G. Rivas, P. H. Bolívar, P. de Maagt, and H. Kurz, "Temperature dependence of the permittivity and loss tangent of high-permittivity materials at terahertz frequencies," *IEEE T. Microw. Theory* **53**, 1266–1271 (2005).
26. Z. Haskal, A. Davis, A. McAllister, and E. Furth, "PTFE-encapsulated endovascular stent-graft for transjugular intrahepatic portosystemic shunts: experimental evaluation," *Radiology* **205**, 682–688 (1997).
27. Y. Takami, T. Nakazawa, K. Makinouchi, J. Glueck, and Y. Nosé, "Biocompatibility of alumina ceramic and polyethylene as materials for pivot bearings of a centrifugal blood pump," *J. of Biomed. Mater. Res.* **36**, 381–386 (1997).
28. R. Simpkin, "Derivation of Lichtenecker's logarithmic mixture formula from Maxwell's equations," *IEEE T. Microw. Theory* **58**, 545–550 (2010).
29. B.-Y. Ung, J. Li, H. Lin, B. M. Fischer, W. Withayachumnankul, and D. Abbott, "Dual-mode terahertz time-domain spectroscopy system," *IEEE Trans. Terahertz Sci. Technol.* **3**, 216–220 (2013).
30. W. Withayachumnankul and M. Naftaly, "Fundamentals of measurement in terahertz time-domain spectroscopy," *J Infrared Millim. Terahertz Wave* **35**, 610–637 (2014).
31. A. Sihvola, "Two main avenues leading to the maxwell garnett mixing rule," *J. Electromagnet. Wave* **15**, 715–725 (2001).
32. J. M. Garnett, "Colours in metal glasses and in metallic films," *Proc. Roy. Soc. Lond.*, pp. 443–445 (1904).
33. H. Looyenga, "Dielectric constants of heterogeneous mixtures," *Physica* **31**, 401–406 (1965).
34. A. Hernandez-Serrano, S. Corzo-Garcia, E. Garcia-Sanchez, M. Alfaro, and E. Castro-Camus, "Quality control of leather by terahertz time domain spectroscopy," *Appl. Opt.* **53**, 7872–7876 (2014).
35. J. Peelen and R. Metselaar, "Light scattering by pores in polycrystalline materials: Transmission properties of

- alumina," J. Appl. Phys. **45**, 216–220 (1974).
36. K. Chenoweth, S. Cheung, A. C. Van Duin, W. A. Goddard, and E. M. Kober, "Simulations on the thermal decomposition of a poly (dimethylsiloxane) polymer using the ReaxFF reactive force field," J. Am. Chem. Soc. **127**, 7192–7202 (2005).
 37. C. Nelson, S. Sant, L. Overzet, and M. Goeckner, "Surface kinetics with low ion energy bombardment in fluorocarbon plasmas," Plasma Sources Sci. T. **16**, 813 (2007).

1. Introduction

Elastomeric polymers such as polydimethylsiloxane (PDMS) [1] are often utilised as dielectric materials for terahertz components, owing to their flexibility and compatibility with microfabrication techniques [2–5]. They can form substrates or spacers to support metallic elements, and the flexibility of these polymers makes it possible to incorporate them into curved, non-planar surfaces, thereby expanding the versatility of electronic [6] and metamaterial devices [7–15]. The bio-compatibility of PDMS in particular makes it a suitable candidate for biomedical terahertz applications [16]. Such polymers, however, have moderate loss in the terahertz range [11,17,18]. Although lower loss dielectric materials such as ceramics and intrinsic semiconductors are available, they are rigid, and not readily compatible with microfabrication. It is possible to modify the material properties of a polymer by introducing powder materials, and this technique has been used in the terahertz range to improve the performance of

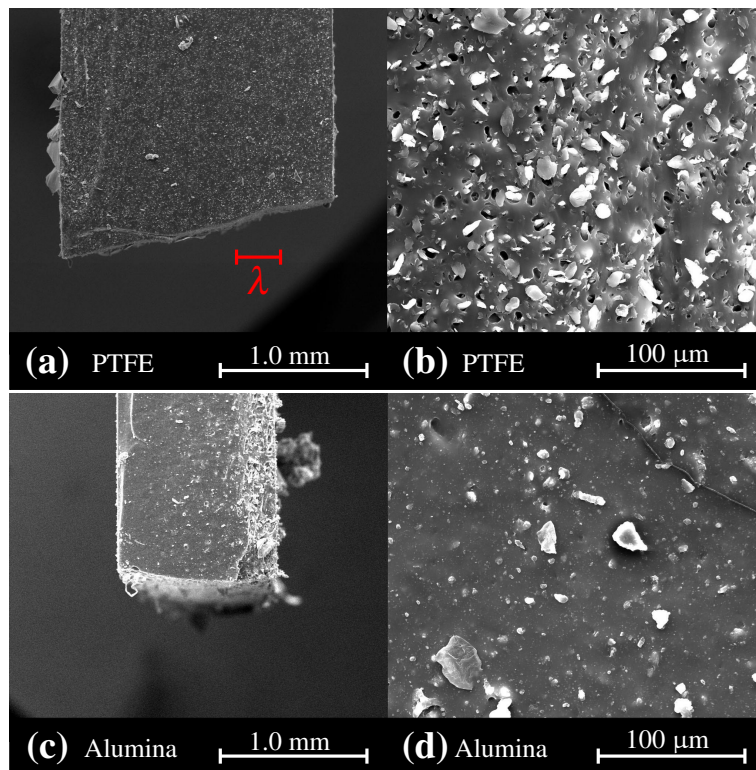


Fig. 1. SEM images of 40%wt PTFE-doped sample at (a) 100 \times and (b) 1000 \times , and the alumina-doped sample at (c) 100 \times and (d) 1000 \times . Scale of wavelength at 1 THz is shown in red in (a).

Dällenbach absorbers [19], to increase the refractive index of a dielectric material at the expense of increased loss [20–22], and to show that terahertz time domain spectroscopy can be used to determine the composition of a sample [23]. However, so far no attempts have been made to produce low-loss effective media for terahertz waves.

In this work we present a technique for reducing the dielectric loss of the elastomeric compound PDMS by combining it with low-loss dopants in order to form an artificial medium, with effective properties determined by the intrinsic properties and fractions of the constituent media. Alumina (Al_2O_3) and polytetrafluoroethylene (PTFE) are selected as dopants as they exhibit low loss in the terahertz range [24, 25]. In pure form, however, these dopants are not suitable for microfabrication techniques. As such, we aim to combine the desirable dielectric properties of low-loss dielectric materials with the desirable mechanical properties of PDMS. Additionally, the inclusion of dopant particles is not expected to compromise the bio-compatibility of PDMS, as alumina and PTFE are both bio-compatible [26, 27].

In brief, the study begins with sample preparation by introducing the powder dopants to the liquid-phase host medium prior to curing. Terahertz time-domain spectroscopy (THz-TDS) is then used to characterise the samples. The results are compared to effective medium theory, using the Lichtenecker logarithmic mixture formula [28].

2. Fabrication and experiment

In order to prepare the samples, a known amount of liquid PDMS, comprising a 1:10 mixture of pre-polymer and a curing agent, is mixed with a known amount of powder dopant in order to yield a desired mass percentage. Liquid composite mixtures are then degassed in a vacuum chamber for a period of two hours in order to extract trapped air bubbles, and then poured

Table 1. Thicknesses of all PDMS samples, as measured with both SEM and micrometer readout, including standard deviations.

Dopant	Concentration by weight	SEM readout (mm)	Micrometer readout (mm)
None	–	4.45 ± 0.10	4.38 ± 0.01
PTFE	10%	1.04 ± 0.03	1.05 ± 0.03
	20%	2.00 ± 0.02	1.92 ± 0.01
	40%	1.94 ± 0.04	2.08 ± 0.01
Alumina	10%	2.08 ± 0.02	1.98 ± 0.01
	20%	1.90 ± 0.05	1.85 ± 0.05
	40%	1.02 ± 0.02	1.01 ± 0.01

Table 2. Extracted material properties at 0.7 THz.

Dopant	Concentration by weight	ϵ_r	$\tan\delta (\times 10^{-2})$	n	$\alpha (\text{cm}^{-1})$
None	–	2.25 ± 0.04	5.88 ± 0.13	1.501 ± 0.014	12.9 ± 0.2
PTFE	10%	2.29 ± 0.01	5.66 ± 0.06	1.515 ± 0.005	12.5 ± 0.2
	20%	2.29 ± 0.01	5.33 ± 0.04	1.512 ± 0.003	11.8 ± 0.1
	40%	2.24 ± 0.01	4.98 ± 0.09	1.498 ± 0.003	10.9 ± 0.2
Alumina	10%	2.42 ± 0.02	5.89 ± 0.06	1.557 ± 0.005	13.4 ± 0.2
	20%	2.56 ± 0.01	5.63 ± 0.09	1.600 ± 0.004	13.2 ± 0.2
	40%	2.82 ± 0.02	5.37 ± 0.17	1.681 ± 0.005	13.2 ± 0.4

onto a planar silicon wafer. The liquid phase elastomer is then cured at room temperature and atmospheric pressure over a period of 48 hours to realise pliable elastomeric materials. Alumina and PTFE particles (Sigma-Aldrich), of ~ 50 nm and < 12 μm , respectively, were utilised as dopants. Samples of 10%, 20%, and 40% of each dopant by mass are prepared, as well as a pure PDMS sample for comparison. Samples are all sectioned into 3×3 cm^2 squares, with thicknesses ranging from 1.0 mm to 4.5 mm.

Scanning electron microscope (SEM) images of the samples that are 40% dopant by weight are given in Fig. 1. Given that the wavelength at 1 THz is 300 μm , the wavelength is greater than the largest particle size by a factor of 25. Hence the samples can be assumed to be homogeneous, and effective medium theory approximations of homogeneity are applicable. Note that the PTFE samples contain voids in the host medium, due to particles being dislodged from the surface at the edge of the sample as a result of sectioning the sample. This effect is limited to the surface, and is therefore negligible.

In terms of microfabrication compatibility, although the doping increases the viscosity of the liquid polymer, the materials remain compatible with microfabrication processes such as spin-coating. Mechanically, the doped samples remain elastic, like PDMS, however their Young's modulus is significantly modified. Doping also makes the PDMS optically opaque, which can compromise manual alignment in multi-layer structures.

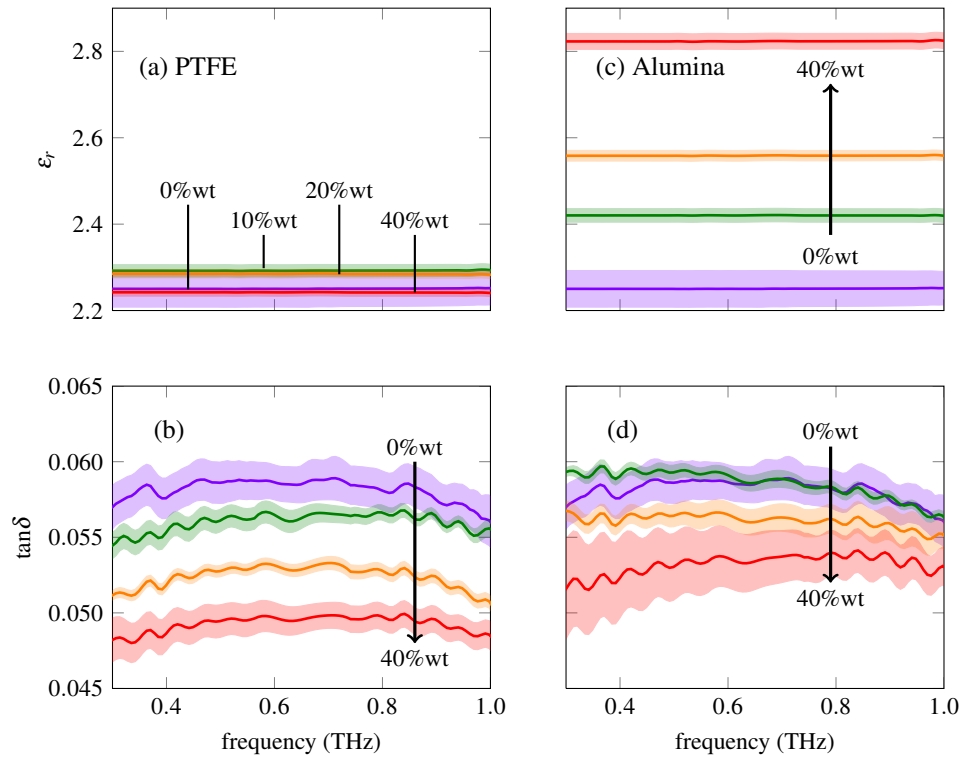


Fig. 2. Material properties of doped PDMS samples, showing: (a) relative permittivity of PTFE-doped samples, (b) loss tangent of PTFE-doped samples, (c) relative permittivity of alumina-doped samples, and (d) loss tangent of alumina-doped samples. The dopant percentage by mass varies from 0%, 10%, 20%, to 40%. Error ranges due to variation in sample thickness and dopant aggregation are indicated with coloured regions.

Samples are characterised using a custom-made photoconductive antenna (PCA)-based THz-TDS system, with off-axis parabolic mirrors to focus the beam onto the sample [29]. The beam waist of the focused beam has a diameter of 2–3 mm. The measurement is carried out in a dry atmosphere, where water vapor absorption is negligible. Given that the samples are flexible and elastic, they are not expected to be of uniform thickness. In order to account for small variation in thickness of the samples, five measurements at random locations are carried out for each sample. This will also account for any fluctuation in dopant concentration within the sample volume.

The thickness of all samples is required in order to extract their material properties. The thickness of each sample is measured using a micrometer, following SEM-based thickness measurement of offcuts at multiple sites. Given the pliable, flexible nature of the samples, due care is taken in order to not exert excessive force on the sample with the micrometer, resulting in readouts from both SEM and micrometer measurements that are in agreement, with values summarized in Table 1.

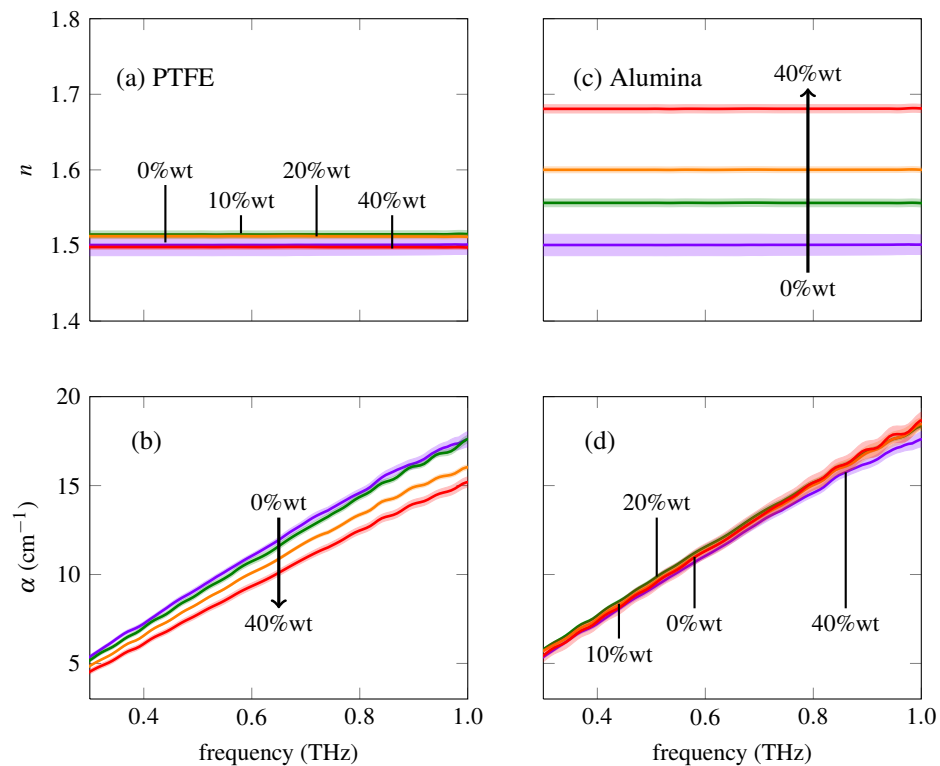


Fig. 3. Material properties of doped PDMS samples, showing; (a) index of refraction of PTFE-doped samples, (b) absorption coefficient of PTFE-doped samples, (c) index of refraction of alumina-doped samples, and (d) absorption coefficient of alumina-doped samples. Error ranges due to variation in sample thickness and dopant aggregation are indicated with coloured regions.

3. Results and discussion

The material properties of all samples tested are extracted, using a standard parameter estimation process [30]. Relative permittivity and loss tangent are presented in Fig. 2, and refractive index and absorption coefficient are presented in Fig. 3. For clarity, material properties at 0.7 THz, where the dynamic range is at maximum, are also presented in Table 2. As expected, the doped samples exhibit a reduction in loss, and samples with higher dopant concentrations exhibit less loss. In addition to reduced loss tangent, samples doped with alumina also exhibit an increase in the relative permittivity. The greatest reduction of loss tangent is achieved with the sample that is doped with 40% PTFE by weight. This sample exhibits an average reduction of 15.3% in loss tangent over a range from 0.3 to 1 THz, as compared to pure PDMS. With regards to dispersion characteristics, the refractive indices of all samples presented in Fig. 3 exhibit negligible variation over the relevant frequency range. We therefore conclude that doping has not increased dispersion. Note the slight non-monotonic trend in the relative permittivity of PTFE-doped PDMS can be ascribed to jitter, as the pulse in the employed THz-TDS system has a tendency to drift slightly in time.

There are multiple approaches to effective medium theory modelling, such as the Maxwell-Garnett formula [31, 32] and the Landau-Lifshitz-Looyenga model [33, 34]. However, these techniques are derived for spherical inclusions, and the dopant particles in this case do not conform to any regular geometry, as shown in Fig. 1. For this reason the Lichtenecker logarithmic mixture formula [28] is selected to model the properties of the effective medium, as it is valid for homogenised dielectric mixtures in which the shapes and orientations of the components are randomly distributed. This formula is given in Equation 1, where ϵ_n and $f_{v,n}$ are the complex permittivity and volumetric fraction of the n^{th} constituent medium, respectively, and ϵ_{eff} is the complex permittivity of the overall mixture.

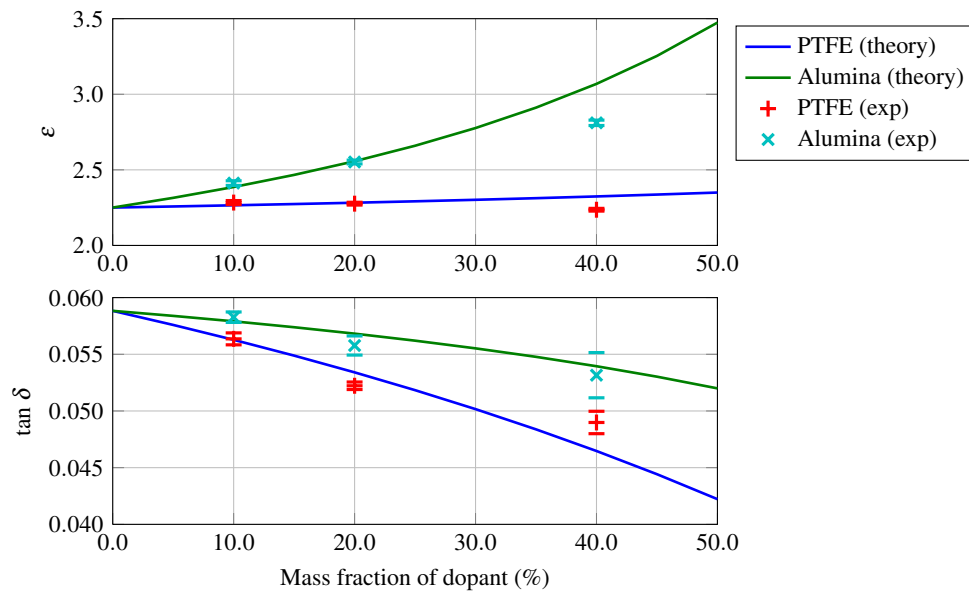


Fig. 4. Comparison of measured results with effective medium theory at 0.7 THz. Error bars on measured results show the measurement uncertainty due to variation in sample thickness.

$$\epsilon_{\text{eff}} = \prod_{n=1}^N \epsilon_n^{f_{v,n}}. \quad (1)$$

In order to apply the Lichtenecker logarithmic mixture formula to the samples under investigation, mass fractions are converted to volumetric fractions using Equation 2, where f_v is the volumetric fraction of the dopant, f_m is the mass fraction of the dopant, ρ_H is the density of the host medium, and ρ_D is the density of the dopant material.

$$f_v = \frac{f_m \rho_H}{f_m \rho_H + (1 - f_m) \rho_D}. \quad (2)$$

Here, the density of PDMS, alumina, and PTFE are $\sim 1.0 \text{ g/cm}^3$, $\sim 4.0 \text{ g/cm}^3$, and $\sim 2.2 \text{ g/cm}^3$ respectively [35–37]. The Lichtenecker logarithmic mixture formula is inverted, and applied to the measured data in order to extract the complex permittivities of the bulk dopants, which are found to be $2.71 + j0.03$ and $21.5 + j0.9$, for PTFE and alumina respectively. The Lichtenecker logarithmic mixture formula is then utilized, using the extracted bulk material properties, to determine the effective permittivity and loss tangent in the continuous range of mass fractions from 0% to 50%, with results given in Fig. 4. This effective medium theory modelling is carried out at 0.7 THz. The results show reasonable agreement with the measured values, with discrepancy being potentially due to agglomeration of dopant particles that compromises the homogenisation of the dielectric.

4. Conclusion

We demonstrate a technique for reducing dielectric loss of elastomeric polymers in the terahertz range by doping with micro/nano-particles. This process gives us the ability to control the dielectric loss tangent, demonstrated by changing it from 0.058 to 0.049 (15.3%) in a sample doped with 40% PTFE by mass. The doped PDMS maintains its compatibility with microfabrication processes. The materials produced could be used as low-loss dielectrics for terahertz components. It is expected that this method will increase the efficiency of polymer-based terahertz metamaterials and biomedical devices. Furthermore, this technique could be extended to other dopants and other polymer/dielectric matrices.

Acknowledgments

We gratefully acknowledge Robiatun Adayiah Awang and Wayne Rowe, RMIT University, for assistance with the selection and preparation of the dopant materials, and Henry Ho, the University of Adelaide, for technical assistance. The authors acknowledge staff and technical assistance at the Australian Microscopy and Microanalysis Research Facility at RMIT University.